Journal of Alloys and Compounds 509 (2011) 5274–5279

Contents lists available at ScienceDirect

Journal of Alloys and Compounds

journal homepage: www.elsevier.com/locate/jallcom

Fabrication of Nd:YAG transparent ceramics with both TEOS and MgO additives

Hao Yang[a,c], Xianpeng Qin[b,c], Jian Zhang[b,c,*], Shiwei Wang[b], Jan Ma[c], Lixi Wang[a], Qitu Zhang[a,**]

[a] College of Materials Science and Engineering, Nanjing University of Technology, Jiangsu Nanjing 210009, China
[b] Shanghai Institute of Ceramics, Chinese Academy of Sciences, Shanghai 200050, China
[c] School of Materials Science and Engineering, Nanyang Technological University, Singapore 639798, Singapore

ARTICLE INFO

Article history:
Received 20 July 2010
Received in revised form 2 November 2010
Accepted 4 November 2010
Available online 13 November 2010

Keywords:
Nd:YAG
Transparent ceramics
Additives
MgO
TEOS

ABSTRACT

Neodymium doped YAG transparent ceramics were fabricated by vacuum reactive sintering method using commercial α-Al_2O_3, Y_2O_3 and Nd_2O_3 powders as the starting materials with both tetraethyl orthosilicate (TEOS) and MgO as sintering aids. The morphologies and microstructure of the powders and Nd:YAG transparent ceramics were investigated. Fully dense Nd:YAG ceramics with average grain size of ~10 μm were obtained by vacuum sintering at 1780 °C for 8 h. No pores and grain-boundary phases were observed. The in-line transmittance of the ceramic was 83.8% at 1064 nm.

1. Introduction

Neodymium doped yttrium aluminum garnet (Nd:YAG) has been proven to be one of the best solid-state laser materials in previous research [1,2]. Its indisputable dominance in a broad variety of laser applications is determined by a combination of high emission cross section with long spontaneous emission life-time, high damage threshold, good mechanical strengths, high thermal conductivity and consequently low thermal distortion of the laser beam, etc. [3–6].

Ikesue et al. were the first to demonstrate the possibility of elaborating transparent Nd:YAG ceramics with the required optical properties for laser applications [7,8]. Since then, polycrystalline transparent Nd:YAG ceramics have attracted much attention because the optical quality has been improved greatly. Many recent works have shown that transparent Nd:YAG ceramics are equivalent to or even better than a single crystal grown by the Czochralski method [9–11]. Usually, Nd:YAG transparent ceramics can be fabricated by reactive sintering method using highly purity commercial Al_2O_3, Y_2O_3 and Nd_2O_3 powders as raw materials [7]. Because of low sintering activity of commercial powders, some additives are necessary in the sintering process. It is well known that the use of TEOS as sintering aid is required to reach fully dense and transparent Nd:YAG ceramics by removing the microstructural heterogeneities such as pores and secondary phases [12–14]. However, in our practical work, it is hard to prepare high quality Nd:YAG transparent ceramics only using TEOS as sintering aid if commercial oxide powders were used as the staring materials. MgO is a kind of cheap and common sintering aid for fabricated ceramics which has been successfully applied to fabricate translucent Al_2O_3 ceramics [15,16]. The addition of MgO can inhibit the abnormal grains growth and is helpful to eliminate the residual pores. For YAG transparent ceramics, results for single-added TEOS or MgO as sintering aid have been reported so far [17,18]. However, it is surprising that few researches reported the detail effects of using TEOS and MgO combination as the sintering aids for fabricating YAG based ceramics.

In the present work, Nd:YAG transparent ceramics were fabricated by solid-state reaction and vacuum sintering using high purity α-Al_2O_3,Y_2O_3 and Nd_2O_3 as raw materials with both TEOS and MgO as sintering aids. For Comparison purpose, the Nd:YAG transparent ceramics either with TEOS or with MgO as sintering aid were also prepared. The morphologies and microstructure of the nanopowders and Nd:YAG transparent ceramics were investigated. The effect of sintering temperature and different quantity of sintering aids on the optical properties of transparent ceramics was also studied.

2. Experimental procedures

High-purity powders of α-Al_2O_3 (99.99% purity, Shanghai Wusong Chemical Co., Ltd), Y_2O_3 (99.999% purity, Jiahua Advanced Material Resources Co.,

* Corresponding author at: School of Materials Science and Engineering, Nanyang Technological University, Singapore 639798, Singapore. Tel.: +65 67906835; fax: +65 67909081.
** Corresponding author. Tel.: +86 25 83587246; fax: +86 25 83587246.
E-mail addresses: jianzhang@ntu.edu.sg (J. Zhang), njzqt@126.com (Q. Zhang).

0925-8388/$ – see front matter © 2011 Published by Elsevier B.V.
doi:10.1016/j.jallcom.2010.11.030

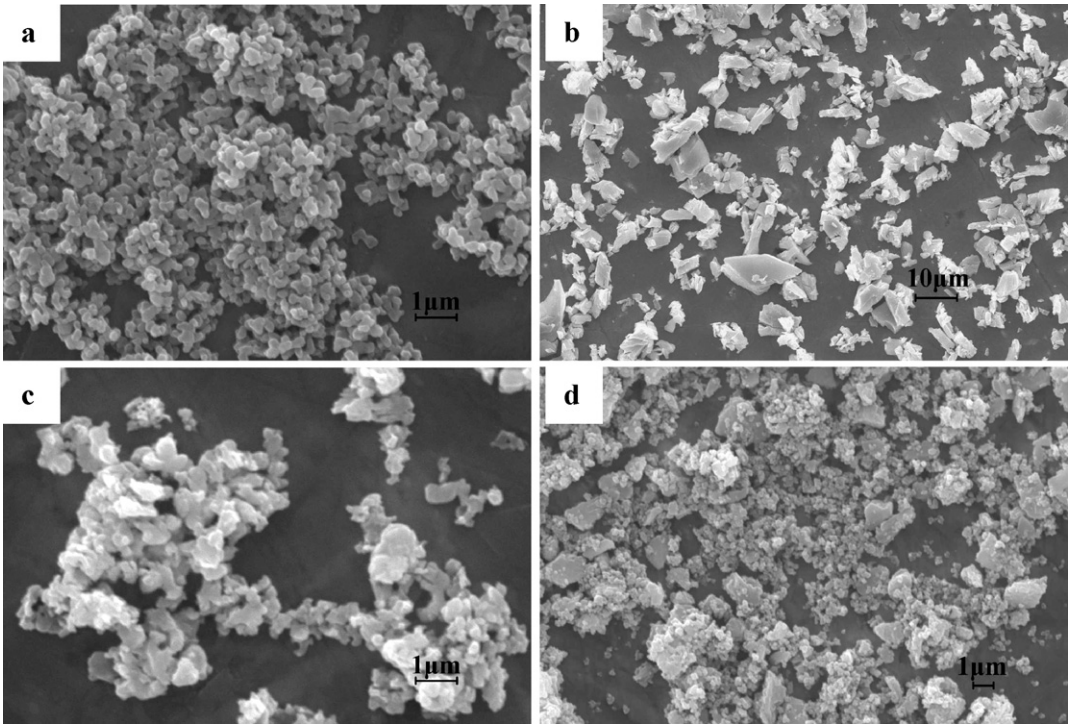

Fig. 1. SEM morphology of starting powders (a) α-Al_2O_3, (b) Y_2O_3, (c) Nd_2O_3 and (d) powder mixture after ball milling.

Ltd) and Nd_2O_3 (99.995% purity, Jiahua Advanced Material Resources Co., Ltd) were used as starting materials, which were all commercially available powders. Five compositions, TS (Nd:YAG + 0.5 wt.% TEOS), T0M(Nd:YAG + 0.1 wt.% MgO), T3M(Nd:YAG + 0.3 wt.% TEOS + 0.1 wt.% MgO), T5M(Nd:YAG + 0.5 wt.% TEOS + 0.1 wt.% MgO) and T8M(Nd:YAG + 0.8 wt.% TEOS + 0.1 wt.% MgO), were designed. These powders were blended together according to the stoichiometric ratio of 1.0 mol.% Nd:YAG and were ball-milled with high-purity Zirconia ball for 12 h in ethanol. The mixture of powders was dried and sieved through a 200-mesh screen. After removing the organic component by calcining at 800 °C for 3 h, the powders were pressed into pellets in a stainless steel die at ~15 MPa. The green body was further cold-isostatically pressed at 200 MPa. The compacted pellets were sintered under vacuum of around 10^{-3} Pa in a furnace equipped with tungsten mesh as the heating element. After that, the pellets were annealed at 1450 °C for 10 h in air and mirror polished on both surfaces. Finally, the size of the Nd:YAG transparent ceramics is Ø 16 mm × 3 mm.

The phase composition of the specimen was identified by X-ray diffraction (XRD, Model D5005, Siemens). Sintered density was measured by the Archimedes method, using deionized water as the immersion medium. The morphologies of starting powders and microstructure of the polished surface of the transparent ceramics were observed by scanning electron microscopy (SEM, JSM-6360LV, JEOM, Tokyo, Japan). Mirror-polished samples on both surfaces were used to measure optical transmittance by a UV–VIS spectrometer (Model U-2800 Spectrophotometer, Hitachi, Tokyo, Japan). The photoluminescence (PL) spectra was measured at room temperature by spectrofluorometer (Fluorolog-3, Jobin Yvon, France), with an 808 nm diode laser used as the pump source.

3. Results and discussion

Fig. 1 shows the SEM morphologies of the starting powders before and after ball milling. The α-Al_2O_3 powders were uniform with a narrow particle size distribution and fairly well dispersed. The average particle size of the α-Al_2O_3 powders was ~500 nm in diameter. The Y_2O_3 powders were relatively wide distribution from submicron to micron in scale and the mean particle size was about ~5 μm. The primary powders of Nd_2O_3 were fine, but they were formed into agglomerates of ~1 μm. The large particles of Y_2O_3 and the fine particles of α-Al_2O_3 and Nd_2O_3 were homogeneously mixed after ball milling.

There are a lot of literature discussing the phase evolution during the sintering [8,13,19]. Generally, it is not possible to get the pure YAG phase from the direct reaction between Y_2O_3 and Al_2O_3 powders during the sintering. Intermediate phases, like $Y_4Al_2O_9$ (YAM) and $YAlO_3$ (YAP) are commonly found during reaction. At the temperature higher than 1400 °C, the YAG phase will start to form. In the present work, the similar reaction sequence has been observed. Fig. 2 shows the XRD pattern of Nd:YAG transparent ceramics sintered at 1780 °C. All the peaks of TM, T5M and TS can be well indexed as the cubic garnet structure of YAG. This indicated that full transformation to YAG occurred during the vacuum sintering.

Fig. 3 shows the transmittance of TS and T0M. The transmittance of TS was much higher than that of T0M in the long wavelength region. The maximum transmittance was 76.9% for TS and 48.2% for T0M at the lasing wavelength of 1064 nm respectively. It could be seen clearly that the transmittance of TS decreased sharply with a decrease in wavelength, especially in the wavelength ranging from 500 to 300 nm. The transmittance was only 42.7% for TS at 400 nm. It is obviously that the decrease of TS was mainly due to the inhomo-

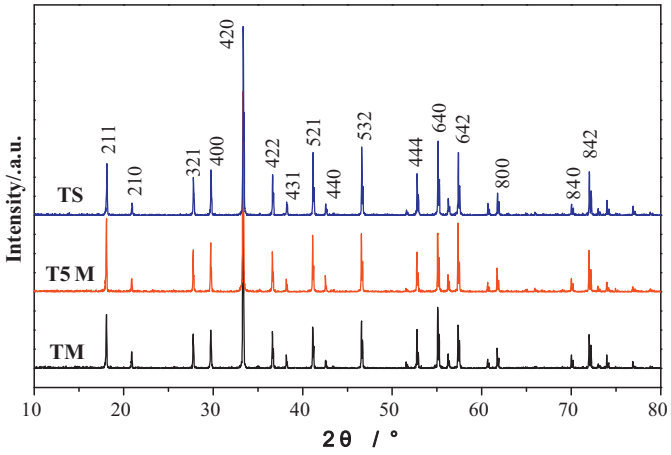

Fig. 2. XRD pattern of Nd:YAG transparent ceramics with TM, T5M and TS.

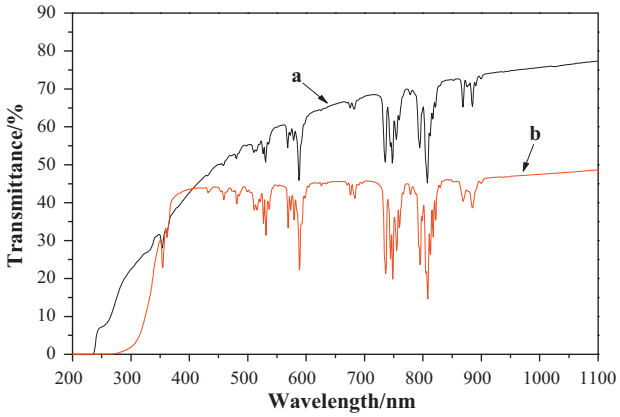

Fig. 3. Optical transmittance spectrum of Nd:YAG samples with (a) TS and (b) T0M.

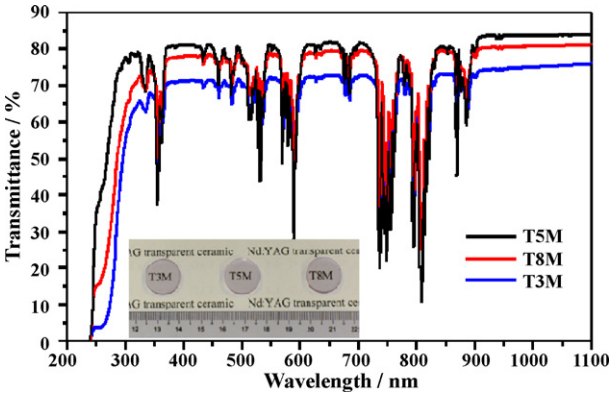

Fig. 5. Photograph and optical transmittance spectrum of Nd:YAG samples with T5M, T8M and T3M.

geneity in different grains and small residual pores in the ceramic which can be found from Fig. 4(B1). Compared with TS, the transmittance of T0M decreased less in the measure region though the maximum transmittance was not high. It still reached 43.5% even at 400 nm and the total drop down is less than 10%. According to the transmittance, it is indicated that the grains of T0M should be uniform.

Fig. 4 shows the SEM micrographs of the sample. Grain size, grain boundary phase and pores are usually considered as the main factors affecting transmittance of ceramics [20,21]. As shown in Fig. 4(A1), the average grain size of the TS was about 30 μm. Apparently, no grain-boundary phases existed in the microstructure of the TS ceramic. However, severe abnormal grain growths were observed, and several pores were trapped into the grain which can be observed in figure. The size of the pores is around 2 μm. These trapped pores will work as the scattering centre and greatly reduce the optical transmittances in the region of short wavelength. Fig. 4(A2) shows the microstructure of fractured surface of TS. It could be seen that the fracture mode is transgranular in the large grain area and intergranular in the small grain area. As shown in Fig. 4(B1), the grain size of T0M sample was homogeneous and about 3 μm in average. It is much smaller than that of TS. However, the grains were not packed densely on each other. Many pores existed in the triangle grain boundaries. It can be seen clearly in the partial magnified micrograph of Fig. 4(B1). That is the reason why the transmittance of T0M kept in low level through the measure region. The microstructure of fractured surface of T0M is shown in Fig. 4(B2). The fracture mode was absolutely intergranular.

The transmittance of Nd:YAG samples with 0.1 wt.% MgO and different quantity of TEOS is shown in Fig. 5. Obviously, the transmittance of T5M was the best of all. Moreover, the samples with compound MgO and TEOS as sintering aids owned better trans-

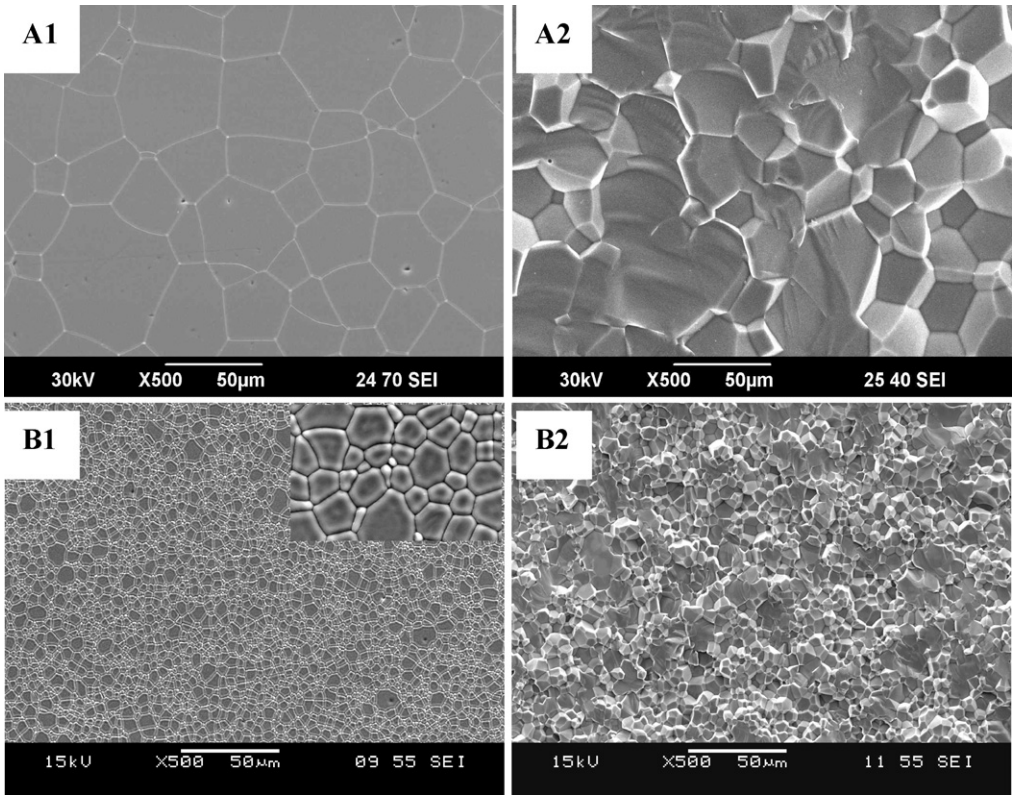

Fig. 4. SEM micrographs of the mirror-polished surface and fractured surface of samples with (A1) and (A2) TS and (B1) and (B2) T0M.

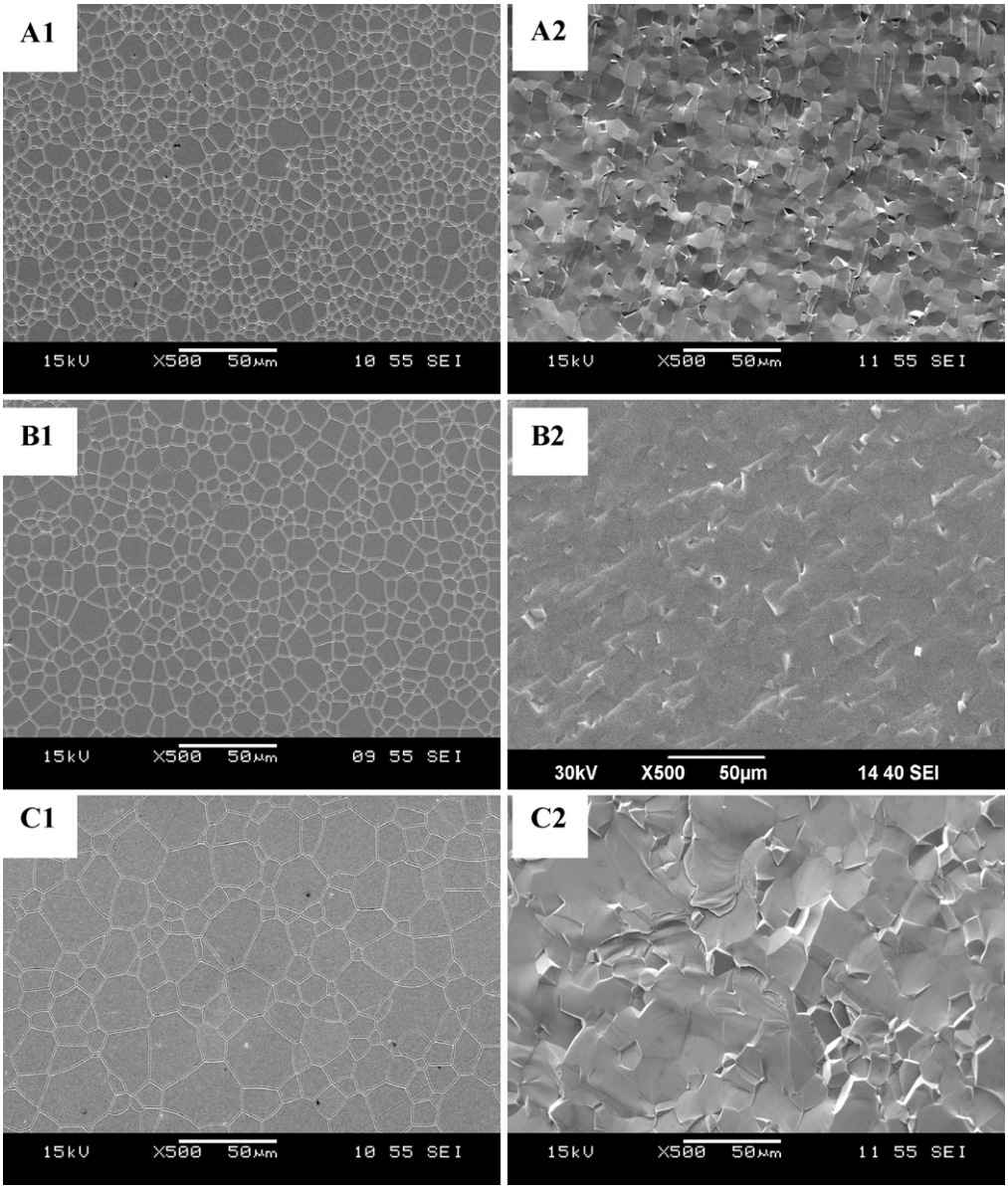

Fig. 6. SEM micrographs of the mirror-polished surface and fractured surface of samples with (A1) and (A2) T3M, (B1) and (B2) T5M, (C1) and (C2) T8M.

mittance than that of TS and T0M which only use TEOS or MgO as the sintering aid. The maximum transmittance was 83.8% for T5M, 80.9% for T8M and 75.6% for T3M at 1064 nm respectively. The transmittance of sample T8M is only a little lower than that of sample T5M. The transmittance of all samples decreased less in the region from 1100 to 400 nm.

Fig. 6 shows the SEM micrographs of samples with different quantity of TEOS. It is seen clearly that the average grain size increased with the increasing doping amount of TEOS. Especially for T8M sample, the grain size is obviously larger than those of the other samples. All of the fracture modes of three samples were transgranular.

Fig. 7 shows the transmittance of T5M under different sintering temperatures. The transmittance of samples sintered at 1720 °C and 1740 °C decrease sharply with the wavelength shifting towards to short wavelength region. The samples sintered at 1760 °C and 1780 °C have the similar transmittance in the measured region. However, the transmittance of sample sintered at 1780 °C is better than that sintered at 1760 °C. It indicated that the best sintering temperature is 1780 °C.

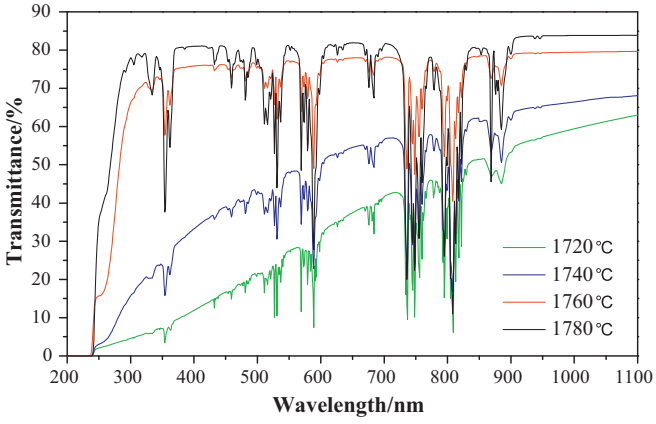

Fig. 7. Optical transmittance spectrum of Nd:YAG samples sintered at different temperatures.

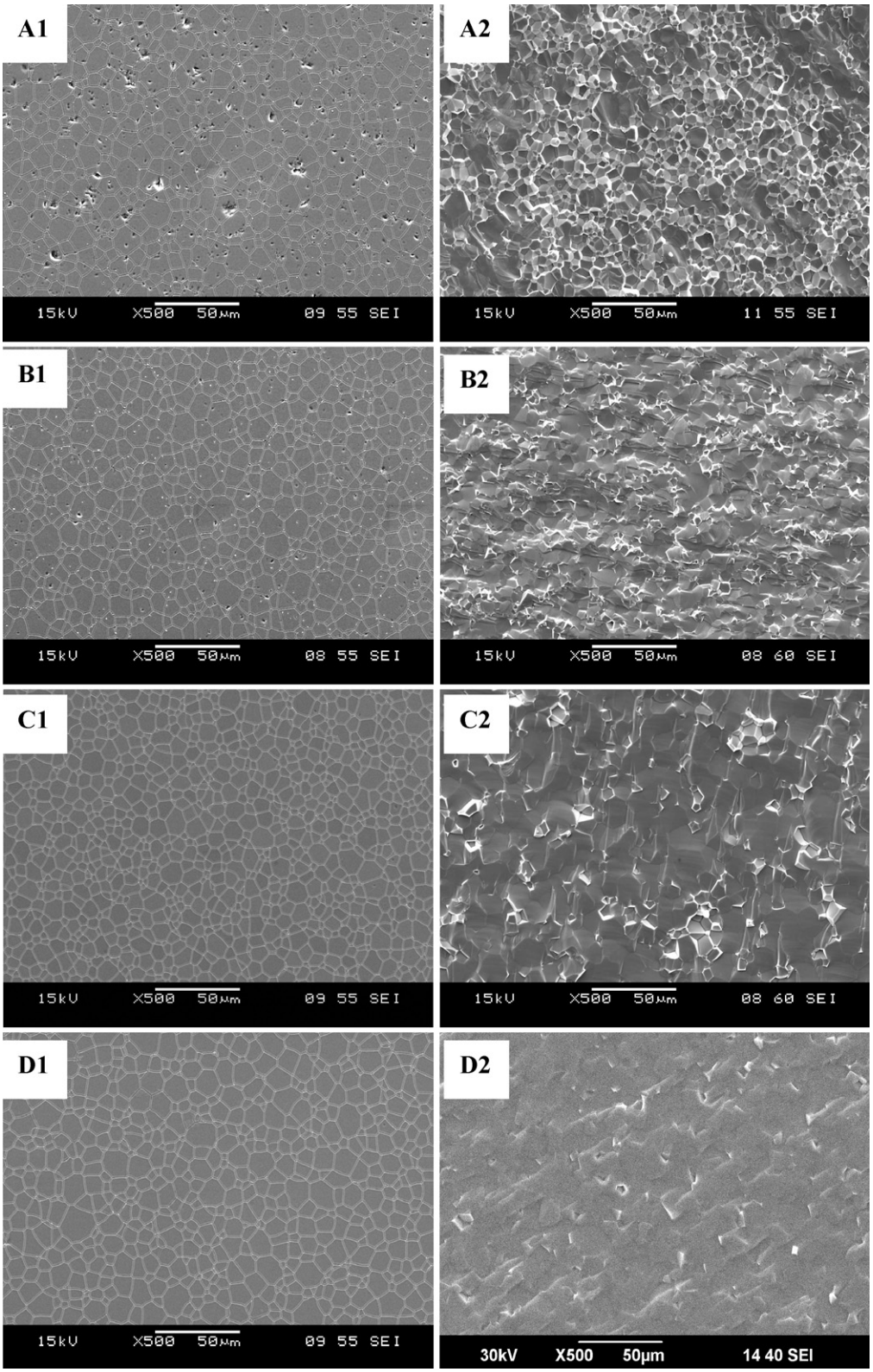

Fig. 8. SEM micrographs of the mirror-polished surface and fractured surface of samples with (A1) and (A2) 1720 °C, (B1) and (B2) 1740 °C, (C1) and (C2) 1760 °C, (D1) and (D2) 1780 °C.

Fig. 8 shows SEM micrographs of Nd:YAG ceramics sintered at 1720–1780 °C for 8 h. It could be seen that the grain size increased less with increase of sintering temperature and the average grain size was about 10 μm. However, the residual pores were gradually removed as the sintering temperature increased. For the sample sintered at 1720 °C (Fig. 8(A1)), quite a few pores were remained inside the grains and between the grain boundaries. A full dense and pore-free microstructure was observed at 1780 °C (Fig. 8(D1)). The fracture modes of the samples were changed from intergranular to transgranular as the sintering temperature increased from 1720 °C

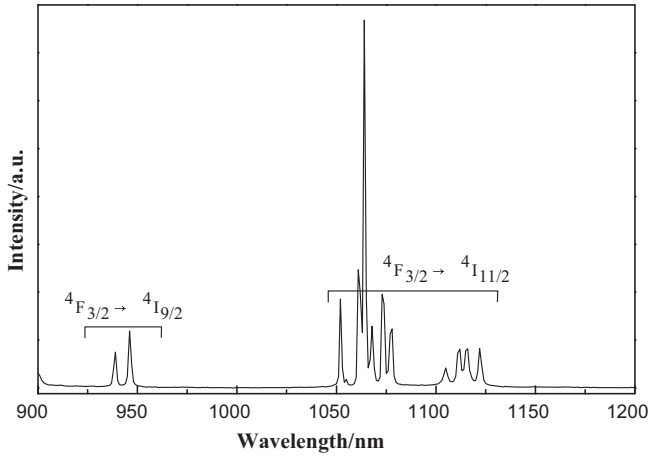

Fig. 9. Photoluminescence spectra of Nd:YAG transparent ceramic.

to 1780 °C. And the fracture mode of the sample sintered at 1780 °C was absolutely transgranular.

The room temperature photoluminescence spectra of 1.0 mol% Nd:YAG transparent ceramic sintered at 1780 °C for 8 h is shown in Fig. 9. From 900 nm to 1200 nm, there are two emission bands centred at 946 nm and 1064 nm, which is corresponding to the transition from $^4F_{3/2} \rightarrow {}^4I_{9/2}$ and $^4F_{3/2} \rightarrow {}^4I_{11/2}$ of Nd^{3+} ions respectively. The main emission peak was at 1064 nm.

The effect of SiO_2 on the sintering is very complex and has been discussed in the literature [13,14,22]. In our research, the combination using of MgO and SiO_2 can greatly enhance the densification for YAG ceramics. Obviously, the addition of minor amounts of MgO as sintering aid to Nd:YAG inhibits the grain growth during sintering and allows the sintering process to proceed to theoretical density. In addition to the effect of SiO_2, the effect of MgO as the sintering aids was investigated as follows:

(a) MgO is segregated as solute at the grain boundaries where it then exerts a drag on grain-boundary motion [23]. The segregation of solute causes a decrease in the grain-boundary mobility, and then inhibits the discontinuous grain growth. And the small amounts of MgO can be used as an inhibitor for liquid phase epitaxy growth of garnet [24].

(b) The effect of MgO could also result in a solid solution formation by substitution of Al^{3+} by Mg^{2+} as follows:

$$2MgO \xrightarrow{Al_2O_3} 2Mg'_{Al} + V_O^{\bullet\bullet} + 2O_O^{\times} \quad (1)$$

According to Eq. (1), one expects that the formation of oxygen vacancies improves the volume diffusion coefficient and could proceed the vacancies diffuse from the pore to the grain boundaries. The vacancies are eliminated at the grain boundaries, causing the enhanced densification rate.

(c) Moreover, there would be another more complex mechanism while using both TEOS and MgO as composite sintering aids. According to $MgSiO_3$ system [18,25], the MgO–SiO_2 liquid phase would be formed at the temperature as low as 1380 °C. It is very possible to form the small amount of the liquid phase during the sintering if the combination of TEOS and MgO are used. Probably this small amount of low-melting-point liquid enhanced the densification rate of the Nd:YAG ceramics.

4. Conclusions

High quality transparent Nd:YAG ceramics were fabricated by reactive sintering method and vacuum sintering using commercial powders as raw materials with both TEOS and MgO as sintering aids. Fully dense ceramic consists of uniform grains with the average grain size of 10 μm which distribute homogeneously. The maximum transmittance was 83.8% at the lasing wavelength of 1064 nm. The addition of MgO inhibits the grain growth during sintering and allows the sintering process to proceed to theoretical density. Obviously, the Nd:YAG transparent ceramic with TEOS and MgO as sintering aids is possible to obtain 1064 nm laser output.

Acknowledgements

This work was supported by Jiangsu Province Natural Sciences fund (BK2007724) and Nanjing University of Technology PhD Thesis Innovation Fund (BSCX200902) and NSFC (50902139).

References

[1] A. Ikesue, Opt. Mater. 19 (2002) 183.
[2] T.D. Huang, B.X. Jiang, Y.S. Wu, J. Li, Y. Shi, W.B. Liu, Y.B. Pan, J.K. Guo, J. Alloys Compd. 478 (2009) L16.
[3] H. Yagi, T. Yanagitani, T. Numazawa, K. Ueda, Ceram. Int. 33 (2007) 711.
[4] T. Tachiwaki, M. Yoshinaka, K. Hirota, T. Ikegami, O. Yamaguchi, Solid State Commun. 119 (2001) 603.
[5] J.R. Lu, K. Ueda, H. Yagi, T. Yanagitani, Y. Akiyama, A.A. Kaminskii, J. Alloys Compd. 341 (2002) 220.
[6] J. Li, Y.S. Wu, Y.B. Pan, W.B. Liu, L.P. Huang, J.K. Guo, Opt. Mater. 31 (2008) 6.
[7] A. Ikesue, I. Furusato, K. Kamata, J. Am. Ceram. Soc. 78 (1995) 225.
[8] A. Ikesue, T. Kinoshita, K. Kamata, K. Yoshida, J. Am. Ceram. Soc. 78 (1995) 1033.
[9] J. Lu, M. Prabhu, J. Song, C. Li, J. Xu, K. Ueda, A.A. Kaminskii, H. Yagi, T. Yanagitani, Appl. Phys. B 71 (2000) 469.
[10] U. Aschauer, P. Bowen, J. Am. Ceram. Soc. 93 (2010) 814.
[11] M. Suarez, A. Fernandez, J.L. Menendez, R. Torrecillas, J. Alloys Compd. 493 (2010) 391.
[12] A. Ikesue, K. Yoshida, T. Yamamoto, I. Yamaga, J. Am. Ceram. Soc. 80 (1997) 1517.
[13] A. Maitre, C. Salle, R. Boulesteix, J.F. Baumard, J. Am. Ceram. Soc. 91 (2008) 406.
[14] S. Kochawattana, A. Stevenson, S.H. Lee, M. Ramirez, V. Gopalan, J. Dumm, V.K. Castillo, G.J. Quarles, G.L. Messing, J. Eur. Ceram. Soc. 28 (2008) 1527.
[15] R.L. Coble, J. Am. Ceram. Soc. 45 (1962) 123.
[16] M. Stuer, Z. Zhao, U. Aschauer, P. Bowen, J. Eur. Ceram. Soc. 30 (2010) 1335.
[17] G. De With, H.J.A. Vandijk, Mater. Res. Bull. 19 (1984) 1669.
[18] Y.K. Li, S.M. Zhou, H. Lin, X.R. Hou, W.J. Li, H. Teng, T.T. Jia, J. Alloys Compd. 502 (2010) 225.
[19] S.H. Lee, S. Kochawattana, G.L. Messing, J.Q. Dumm, G. Quarles, V. Castillo, J. Am. Ceram. Soc. 89 (2006) 1945.
[20] A. Ikesue, K. Kamata, J. Am. Ceram. Soc. 79 (1996) 1927.
[21] X.D. Li, J.G. Li, Z.M. Xiu, D. Huo, X.D. Sun, J. Am. Ceram. Soc. 92 (2009) 241.
[22] R. Boulesteix, A. Maitre, J.F. Baumard, C. Salle, Y. Rabinovitch, Opt. Mater. 31 (2009) 711.
[23] P.J. Jorgensen, J.H. Westbrook, J. Am. Ceram. Soc. 47 (1964) 332.
[24] W.H. De Roode, J.M. Robertson, J. Cryst. Growth 63 (1983) 105.
[25] F.R. Boyd, J.L. England, B.T.C. Davis, J. Geophys. Res. 69 (1964) 2101.